GEANT4 models for nucleon-nucleus cross-sections (NA2 VALSIM) *

G. Folger† and V. Grichine‡

October 1, 2007

Abstract

New models implemented in GEANT4 toolkit for nucleon-nucleus cross-sections in the framework EUDET NA2 VALSIM task are discussed. The predictions of these models are compared with experimental data and other existing GEANT4 models.

*to be submitted to Computer Physics Communication journal
†CERN, Geneva, Switzerland
‡contact person, CERN, Geneva, Switzerland and Lebedev Institute, Moscow, Russia, e-mail:Vladimir.Grichine@cern.ch

1 Introduction

The integral cross-sections for hadronic interactions play an important role in correct simulation of hadronic showers. Verifying the total cross-section and the integral elastic and inelastic cross sections for interaction on different targets is thus important. This verification has been one of the VALSIM tasks during 2006-2007.
In GEANT4 [1] the cross-section definitions are the following : $\sigma_{tot} = \sigma_{in} + \sigma_{el}$, and $\sigma_{in} = \sigma_{prod} + \sigma_{qel}$, where σ_{tot}, σ_{in}, σ_{el}, σ_{prod} and σ_{qel} are total, inelastic, elastic, production and quasi-elastic cross-sections, respectively. GEANT4 has (historically) the following models for hadron-nucleus cross-sections:

1. G4HadronCrossSections class for inelastic and elastic hadron (inelastic and elastic) cross sections inherited from GHEISHA [2].

2. G4Proton/NeutronInelasticCrossSection class for Axen-Wellisch parametrization model. Inelastic cross section only [3].

3. G4QElastic class for elastic cross-section of CHIPS model [4].

These models were verified versus experimental data. The experimental data were taken from IHEP-PDG database, and Dubna set [7, 8]. They showed inaccuracy at low energies and constant-like behavior for high energy range. To improve the hadron-nucleus cross-section accuracy in GEANT4 two new models were implemented:

1. G4Pi/Nucleon NuclearCrossSection class for optical model parametrisation data interpolation for pions/nucleons on nuclei. Total, inelastic and elastic ($\sigma_{el} \equiv \sigma_{tot} - \sigma_{in}$) cross sections are available [5, 6].

2. G4GlauberGribovCrossSection class for total and inelastic (also production and single-diffraction!) hadron cross sections in the spirit of Glauber model with Gribov correction.

Here it is reported on verification of total and inelastic cross-sections for hadrons on different targets as well as on new models (optical model parametrisation data interpolation and simplified Glauber model) implemented in GEANT4 for the description of hadron-nucleus cross-sections.

2 Optical model interpolation

The optical model parametrisation data [5, 6] interpolation is essentially based on quasi-optical model for high energies (T > 2 GeV) and on black disk phenomenology with corrections for low energies. The total, inelastic (and elastic) cross sections are interpolated using:

$$\sigma(T, A) = \pi \left[r_o A^{1/3} + \lambda(T, A) \right]^2 f(T) \phi(A)^{\alpha(T)},$$

where λ is de Brojlie length of projectile in CM system, T is the kinetic energy of projectile in laboratory system, A is the atomic weight, and $r_o \sim 1$ fm. Functions $f(T)$, $\phi(A)$ and $\alpha(T)$ are series like:

$$\sum_i a_i T^{b_i} \quad \text{and} \quad \sum_i a_i A^{b_i}.$$

The model data were tabulated and interpolated in the frame work of GEANT4 toolkit. The general disadvantage of optical models is the prediction of constant cross-sections for very high energies. Experimental data show, however, small relativistic rise of hadron-nucleus cross-sections. For this reason we consider Glauber model for the description of hadron-nucleus cross-sections in the high (more than 100 GeV) energy region.

3 Simplified Glauber model for total and inelastic cross sections

As was mentioned in [9], the Glauber model results in the following relations for the total σ_{tot}^{hA} inelastic σ_{in}^{hA} and elastic σ_{el}^{hA} cross sections of a hadron h on a nuclear target A, respectively:

$$\sigma_{tot}^{hA} = 2\int d^2b \left\{1 - \left\langle \exp\left[-\frac{1}{2}\sigma_{tot}^{hN} T_A^h(b)\right]\right\rangle\right\},$$

$$\sigma_{in}^{hA} = \int d^2b \left\{1 - \left\langle \exp\left[-\sigma_{tot}^{hN} T_A^h(b)\right]\right\rangle\right\},$$

$$\sigma_{el}^{hA} \equiv \sigma_{tot}^{hA} - \sigma_{in}^{hA} = \int d^2b \left|1 - \left\langle \exp\left[-\frac{1}{2}\sigma_{tot}^{hN} T_A^h(b)\right]\right\rangle\right|^2,$$

where b is the impact parameter, σ_{tot}^{hN} is the total cross section of the hadron on a nucleon and $T_A^h(b)$ is the hadron profile function. Here $\langle \ldots \rangle$ means a proper averaging of hadron eigenstates including Gribov inelastic shadowing correction. Applying the light-cone dipole approximation for the correction calculation, one can perform averaging:

$$\left\langle \exp\left[-\sigma_{tot}^{hN} T_A^h(b)\right]\right\rangle = \frac{1}{1 + \sigma_{tot}^{hN} T_A^h(b)}.$$

This explicitly demonstates how Gribov correction makes nuclei more transparent (exponent law $\rightarrow$ power law). Then the cross sections read:

$$\sigma_{tot}^{hA} = \int d^2b \frac{\sigma_{tot}^{hN} T_A^h(b)}{1 + \frac{1}{2}\sigma_{tot}^{hN} T_A^h(b)}, \quad \sigma_{in}^{hA} = \int d^2b \frac{\sigma_{tot}^{hN} T_A^h(b)}{1 + \sigma_{tot}^{hN} T_A^h(b)},$$

For practical calculations in a wide range of hadrons and nuclei, we introduce two simplifications for the hadron profile function $T_A^h(b)$ calculation according to the Glauber model (s corresponds to (x, y)-plane):

$$T_A^h(b) = \frac{2}{\sigma_{tot}^{hN}} \int d^2s \mathrm{Re}\Gamma^{hN}(s) T_A(\vec{b} - \vec{s}), \quad T_A(b) = A\int_{-\infty}^{\infty} d\, z \rho(b, z),$$

where $T_A(b)$ is the nuclear thickness function, A is the number of nucleons in the target nucleus and $\rho(b,z)$ is the nuclear density normalised on unit (z is the distance along the hadron trajectory at the impact parameter b).
The elastic scattering amplitude $i\Gamma^{hN}(s)$ on a nucleon can be used in exponential form:

$$\mathrm{Re}\Gamma^{hN}(s) = \frac{\sigma_{tot}^{hN}}{4\pi B_{hN}} \exp\left(-\frac{s^2}{2B_{hN}}\right),$$

where B_{hN} is the slope of the differential hN elastic cross section. The latter relation can be simplified assuming small slope B_{hN} or small size of a nucleon compared to the nucleous:

$$\mathrm{Re}\Gamma^{hN}(s)\ (B_{hN} \to 0) \to \frac{\sigma_{tot}^{hN}}{2}\delta(x)\delta(y),$$

$$T_A^h(b)\ (B_{hN} \to 0) \sim T_A(b) = A\int_{-\infty}^{\infty} d\,z\rho(b,z),$$

The second step is simplified Gaussian representation of $\rho(b,z)$:

$$\rho(b,z) = \frac{1}{(R\sqrt{\pi})^3} \exp\left\{-\frac{b^2+z^2}{R^2}\right\},$$

where R is the nuclear radius. It allows us to calculate analytically the cross section integrals in respect of b and z.
Then the cross sections read:

$$\sigma_{tot}^{hA} = 2\pi R^2 \ln\left[1 + \frac{A\sigma_{tot}^{hN}}{2\pi R^2}\right],$$

$$\sigma_{in}^{hA} = \pi R^2 \ln\left[1 + \frac{A\sigma_{tot}^{hN}}{\pi R^2}\right].$$

The model is reduced to the selection of σ_{tot}^{hN} and $R(A)$ values. We use the latest edition of PDG [10] and different GEANT4 parametrizations for σ_{tot}^{hN}, including the total cross sections of p, $\bar{p}$, n, $\pi^{\pm}$, $K^{\pm}$ and Σ^- on protons and neutrons.
For known cross sections on proton and neutron, $A\sigma_{tot}^{hN} = N_p\sigma_{tot}^{hp} + N_n\sigma_{tot}^{hn}$, where N_p and N_n are the number of protons and neutrons in the nucleus. The nuclear radius is parametrized by:

$$R(A) = r_o A^{\frac{1}{3}} f(A), \quad r_o \sim 1.1\ fm,$$

where for $A > 21$, $f(A) < 1$, while in the opposite case $3 < A < 21$, $f(A) > 1$ in the limits of 20%. Below in the next section are the model predictions for the nucleon (inelastic, total and elastic) cross sections on different targets.

3.1 Simplified Glauber model cross section ratios

The Glauber approach allows us to estimate the ratios of quasi-elastic and single-diffraction cross-sections to the inelastic cross-section for hadron-nucleus interaction. In the framework of simplified Glauber-Gribov model the cross sections read:

$$\sigma_{tot}^{hA} = 2\pi R^2 \ln\left[1 + \frac{A\sigma_{tot}^{hN}}{2\pi R^2}\right], \quad \sigma_{in}^{hA} = \pi R^2 \ln\left[1 + \frac{A\sigma_{tot}^{hN}}{\pi R^2}\right].$$

$$\sigma_{prod}^{hA} = \pi R^2 \ln\left[1 + \frac{A\sigma_{in}^{hN}}{\pi R^2}\right], \quad \sigma_{qe}^{hA} = \sigma_{in}^{hA} - \sigma_{prod}^{hA}$$

$$\sigma_{sd}^{hA}(hA \to XA) = \pi R^2 \left\{\alpha - \ln\left[1 + \alpha\right]\right\}, \quad \alpha = \frac{A\sigma_{tot}^{hN}}{2\pi R^2 + A\sigma_{tot}^{hN}}.$$

Where σ_{tot}^{hA}, σ_{in}^{hA}, σ_{prod}^{hA}, σ_{qe}^{hA} and $\sigma_{sd}^{hA}(hA \to XA)$ are the total, inelastic, production, quasi-elastic and single-diffraction cross section of a hadron on a nucleus A, respectively. They depend essentially on the total hadron-nucleon cross sections, σ_{tot}^{hN} and now on the inelastic cross section σ_{in}^{hN}. R is the RMS radius of nucleon distribution inside the nucleus.

4 Comparison with experimental data

Comparisons have been undertaken for protons, neutrons, π^+ and π^- on He, C, Fe, Cu, W, Pb, and U targets in the particle energy range $0.1 - 1000$ GeV. One limitations identified of existing GEANT4 cross sections was the dependence of integral cross-sections on energy in the range > 100 GeV. Existing implementations had either a large relativistic rise (G4HadronCrossSections model), or were constant above 100 GeV, according to low energy optical models [6]. A new cross section implementation for total and inelastic hadron integral cross sections was developed, to correct this. It utilizes a simplified version of the Glauber model with Gribov correction (GG model).

Fig. 1 up to Fig. 15 demonstrate the comparisons, and the new 'GG' model, in the integral inelastic and total cross sections of neutrons on carbon target, respectively. At energies above 1 GeV agreement is found with experimental data [7, 8] at a typical level of $10 - 20\%$. The expected small relativistic rise versus energy for the range > 100 GeV is reproduced in the 'GG' model. An additional implementation of integral cross sections for protons and neutrons using Barashenkov's evaluations [6] has been initiated, to account for the low-energy behavior, below 1 GeV.

Quasi-elastic and single-diffraction to inelastic cross-section ratios for protons, neutrons, π^+ and π^- on different targets versus energy are shown in Fig. 16 up to Fig. 19. The prediction of simplified Glauber model is in agreement with the prediction of CHIPS parametrization utilizing another definition of quasi-elastic cross-section based on consideration of the probability of single elastic hadron-nucleon collision inside nucleus.

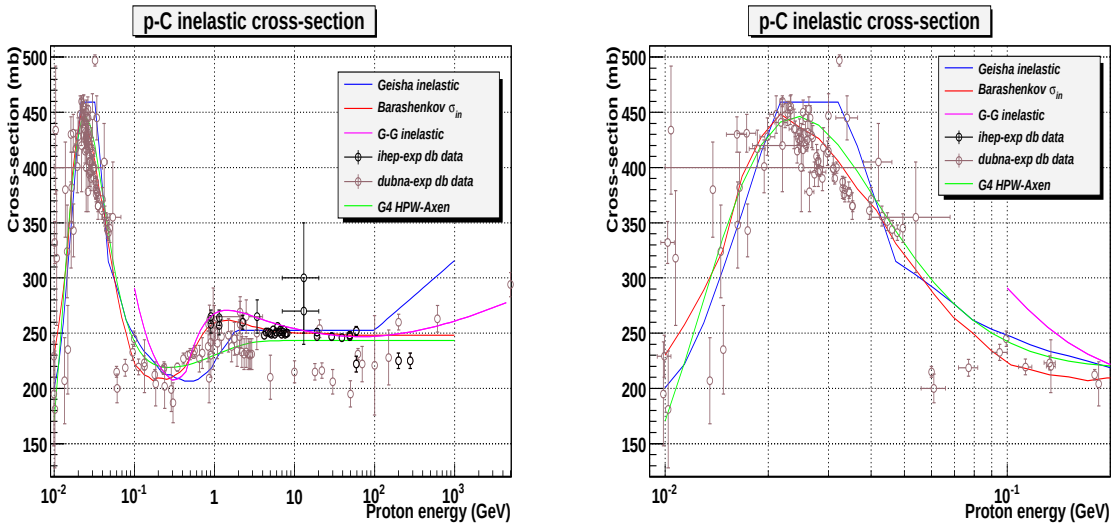

(a) (b)

Figure 1: Integral inelastic cross-sections of protons on carbon target: (a) - 10^{-2} – 10^{3} GeV, (b) - 10^{-2} – 0.2 GeV. Experimental data (open points) from [7, 8], lines correspond to different GEANT4 models.

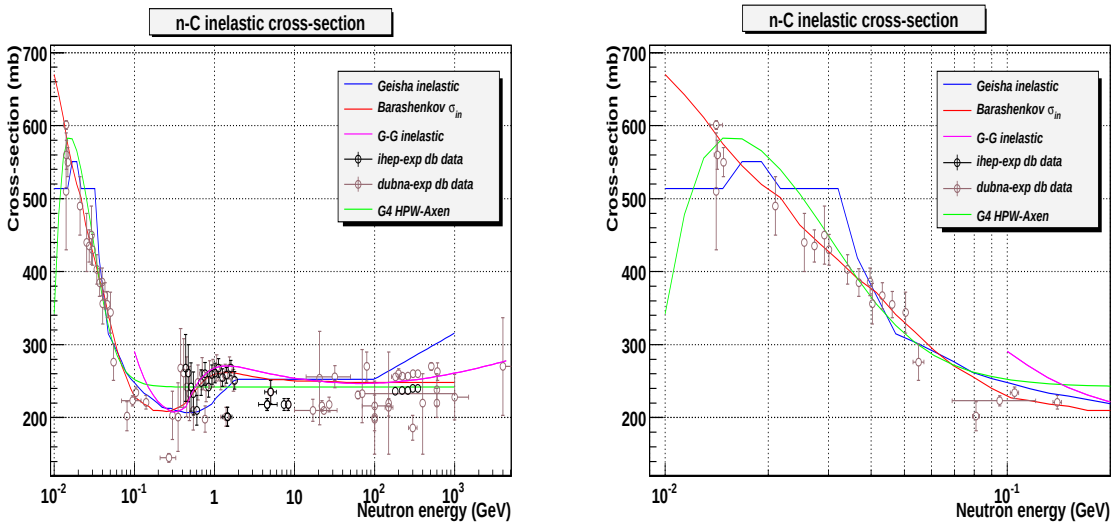

(a) (b)

Figure 2: Integral inelastic cross-sections of neutrons on carbon target: (a) - 10^{-2} – 10^{3} GeV, (b) - 10^{-2} – 0.2 GeV. Experimental data (open points) from [7, 8], lines correspond to different GEANT4 models.

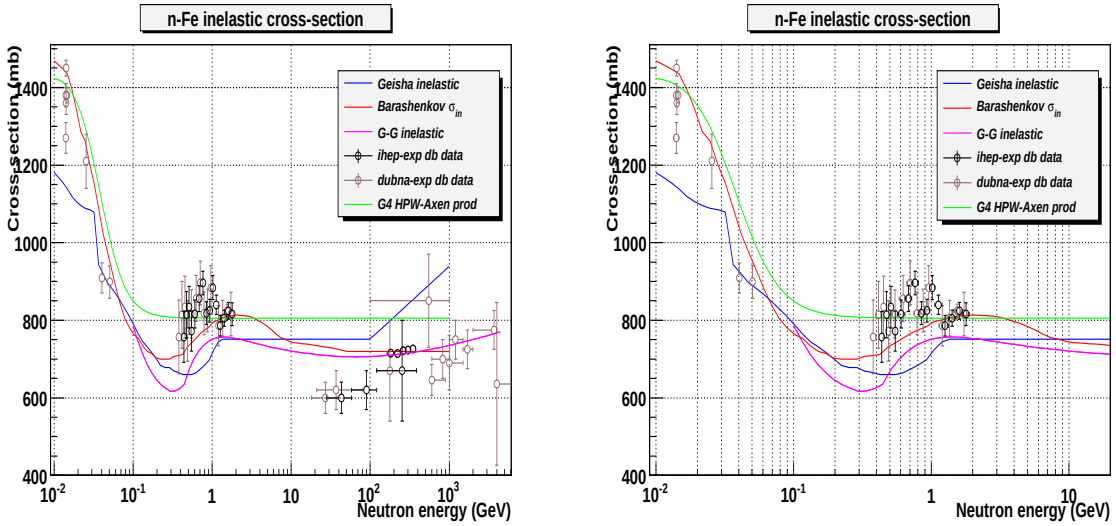

(a) (b)

Figure 3: Integral inelastic cross-sections of neutrons on iron target: (a) - $10^{-2}-10^{3}$ GeV, (b) - $10^{-20}-2$ GeV. Experimental data (open points) from [7, 8], lines correspond to different GEANT4 models.

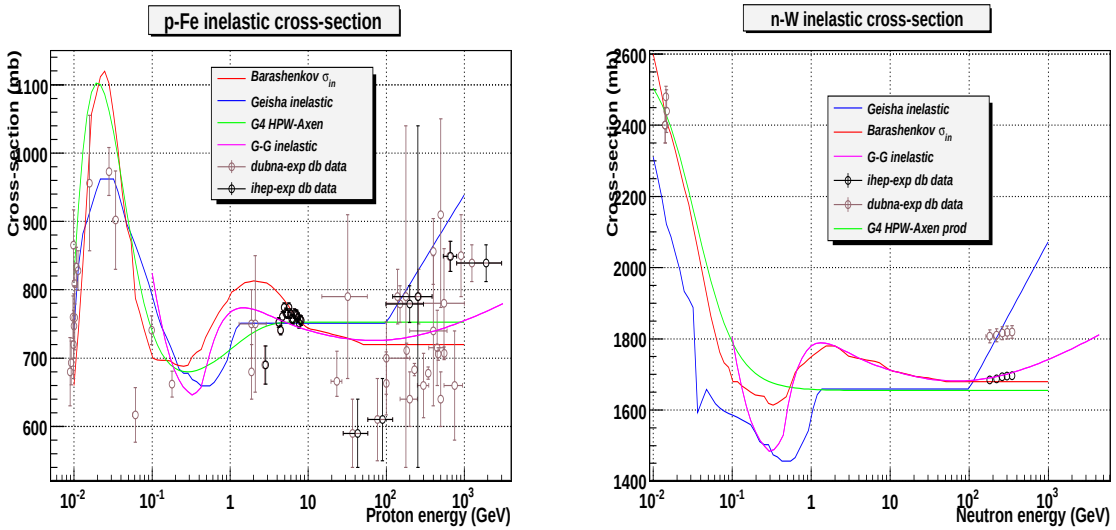

(a) (b)

Figure 4: Integral inelastic cross-sections of of protons on iron (a) and neutrons on tungsten (b) targets. Experimental data (open points) from [7, 8], lines correspond to different GEANT4 models. The data nW for 200-400 GeV are shown with and without quasi-elastic cross-section correction.

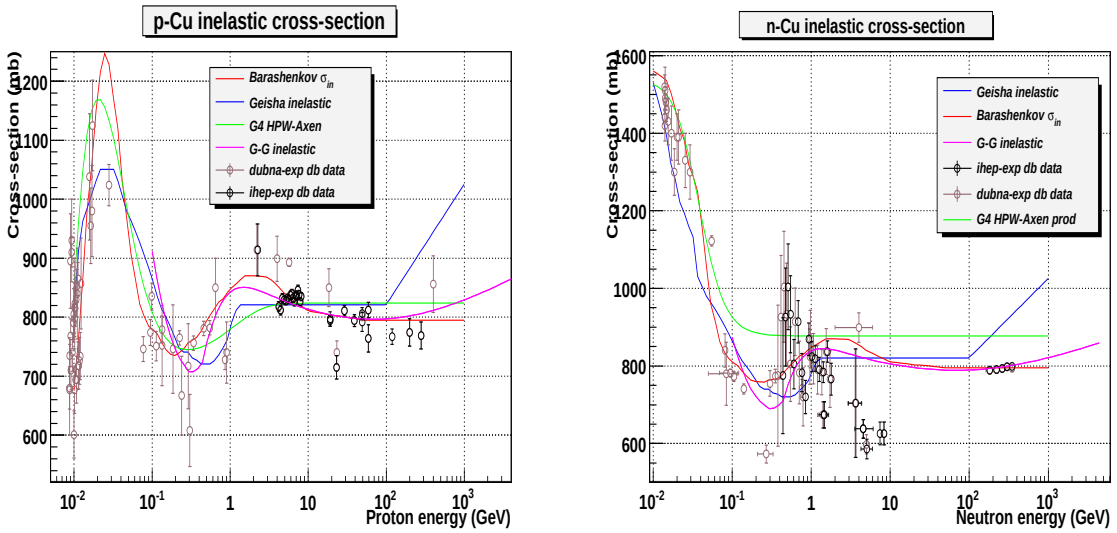

(a) (b)

Figure 5: Integral inelastic cross-sections of of protons (a) and neutrons (b) on copper target. Experimental data (open points) from [7, 8], lines correspond to different GEANT4 models.

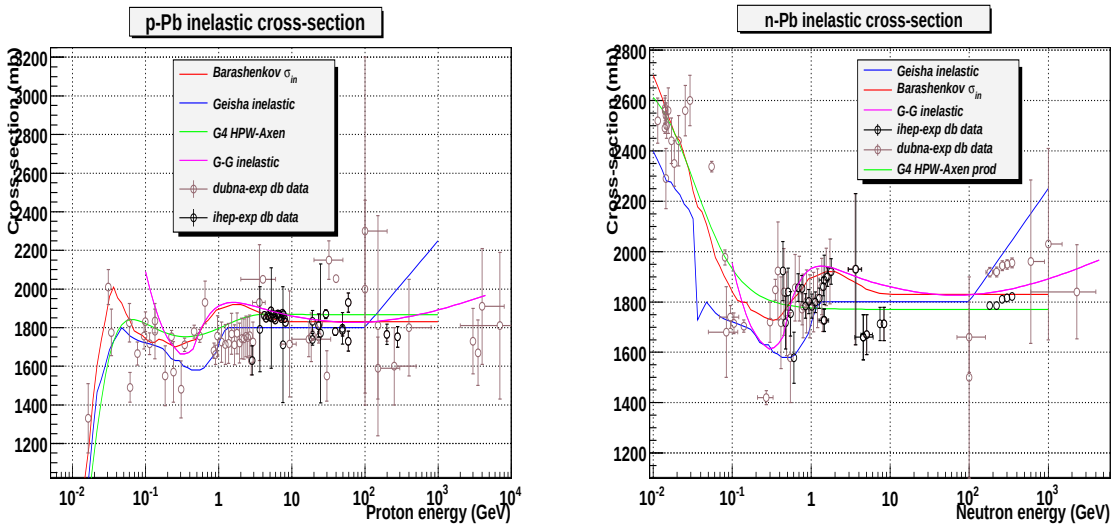

(a) (b)

Figure 6: Integral inelastic cross-sections of of protons (a) and neutrons (b) on lead target. Experimental data (open points) from [7, 8], lines correspond to different GEANT4 models. The data nPb for 200-400 GeV are shown with and without quasi-elastic cross-section correction.

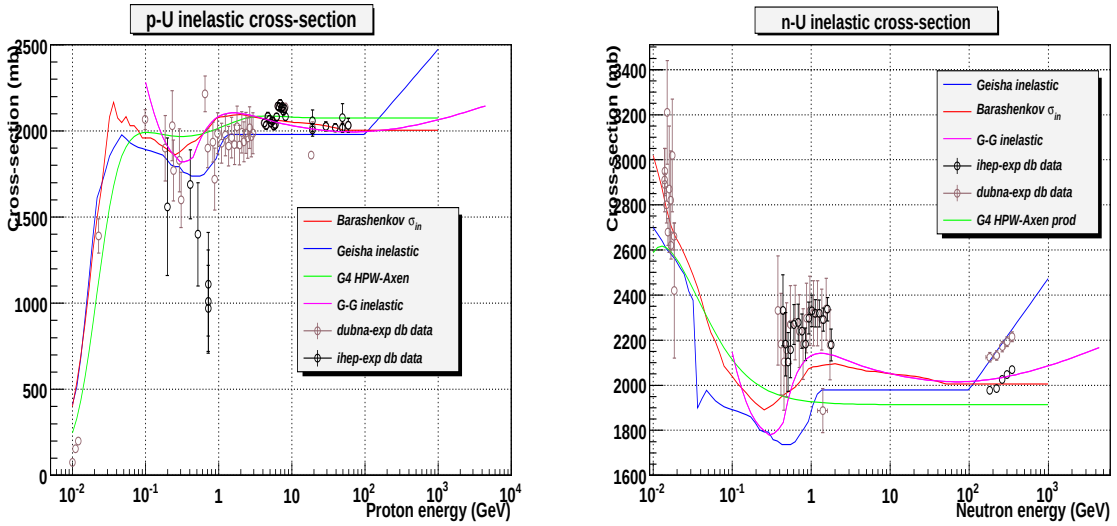

(a) (b)

Figure 7: Integral inelastic cross-sections of of protons (a) and neutrons (b) on uranium target. Experimental data (open points) from [7, 8], lines correspond to different GEANT4 models. The data nU for 200-400 GeV are shown with and without quasi-elastic cross-section correction.

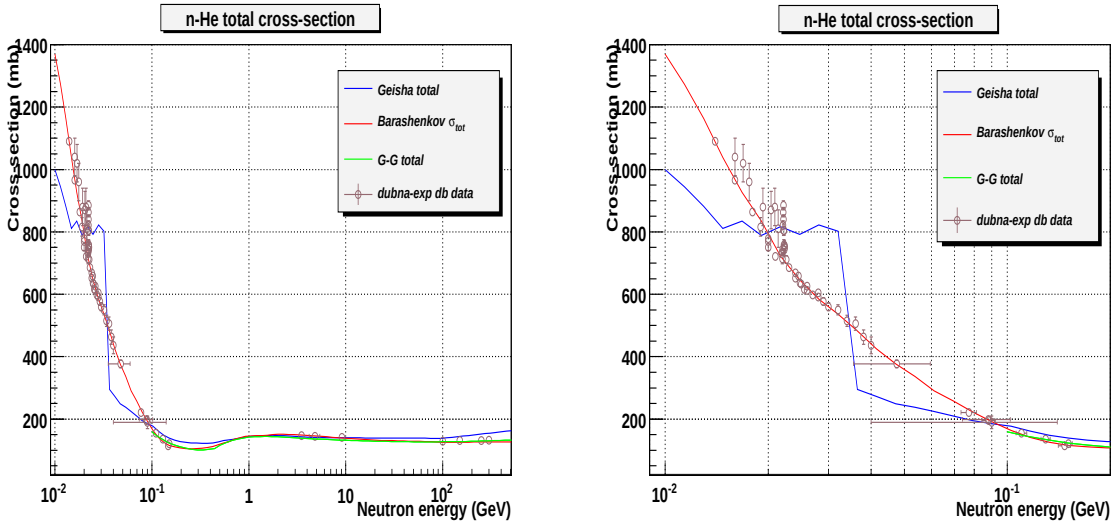

(a) (b)

Figure 8: Integral total cross-sections of neutrons on helium target: (a) - $10^{-2} - 10^{3}$ GeV, (b) - $10^{-2} - 0.2$ GeV. Experimental data (open points) from [7, 8], lines correspond to different GEANT4 models.

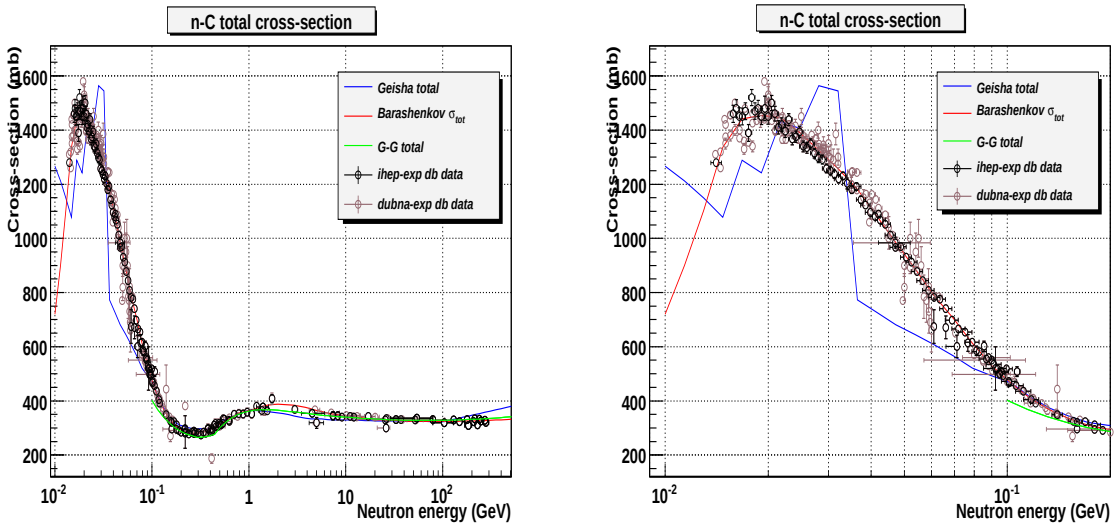

(a) (b)

Figure 9: Integral total cross-sections of neutrons on carbon target: (a) - $10^{-2} - 10^{3}$ GeV, (b) - $10^{-2} - 0.2$ GeV. Experimental data (open points) from [7, 8], lines correspond to different GEANT4 models.

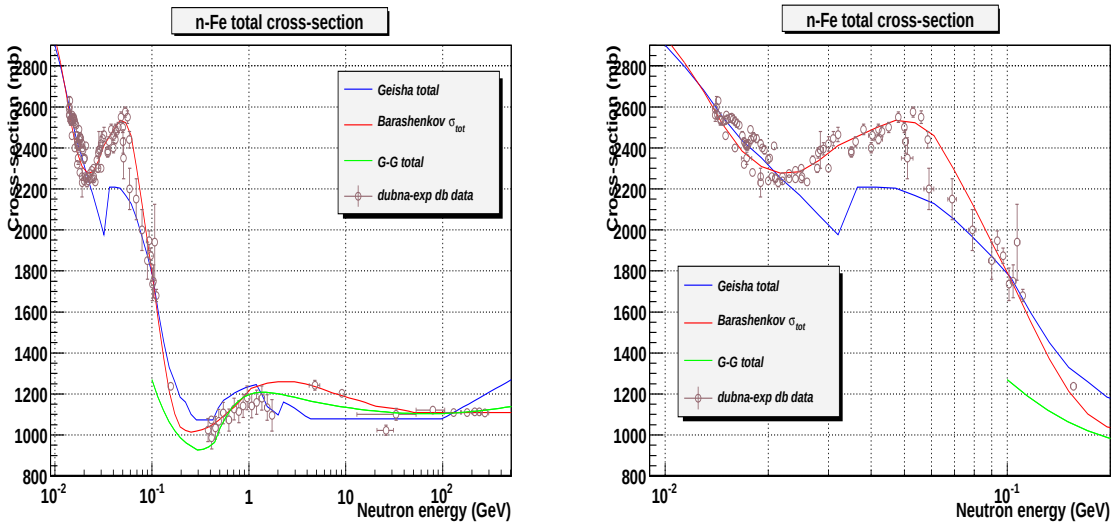

(a) (b)

Figure 10: Integral total cross-sections of neutrons on iron target: (a) - $10^{-2} - 10^{3}$ GeV, (b) - $10^{-2} - 0.2$ GeV. Experimental data (open points) from [7, 8], lines correspond to different GEANT4 models.

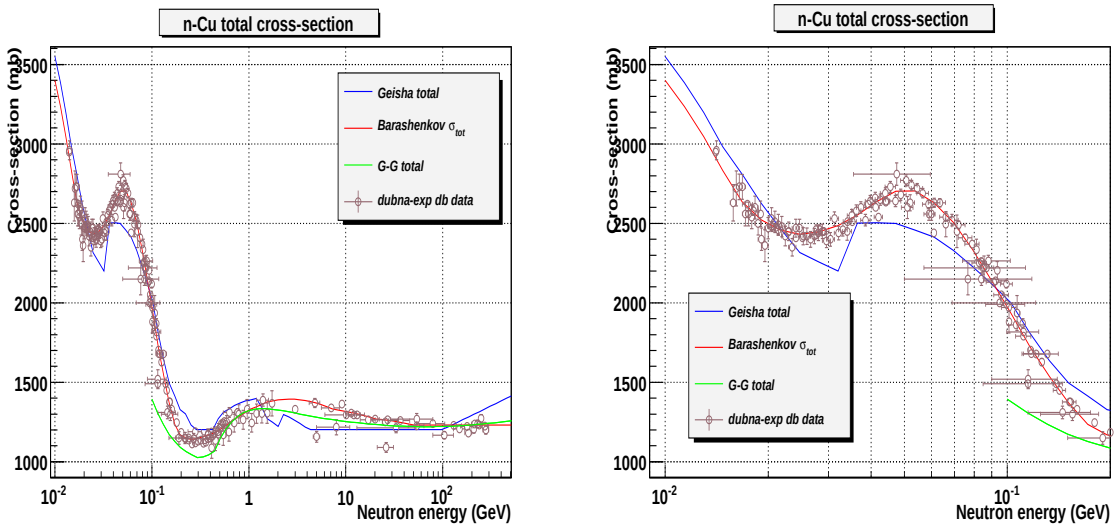

(a) (b)

Figure 11: Integral total cross-sections of neutrons on copper target: (a) - $10^{-2} - 10^{3}$ GeV, (b) - $10^{-2} - 0.2$ GeV. Experimental data (open points) from [7, 8], lines correspond to different GEANT4 models.

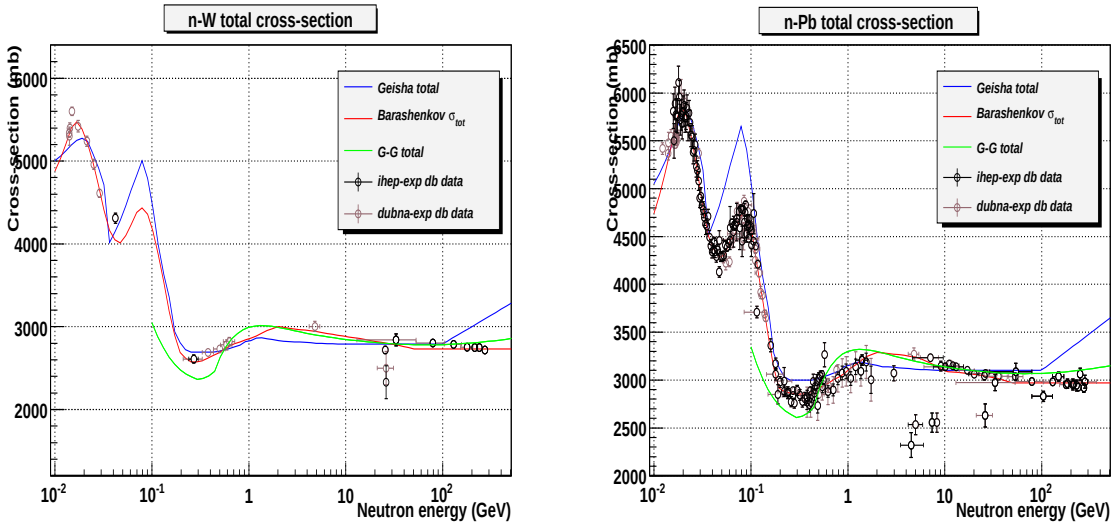

(a) (b)

Figure 12: Integral total cross-sections of neutrons on tungsten (a) and lead (b) targets. Experimental data (open points) from [7, 8], lines correspond to different GEANT4 models.

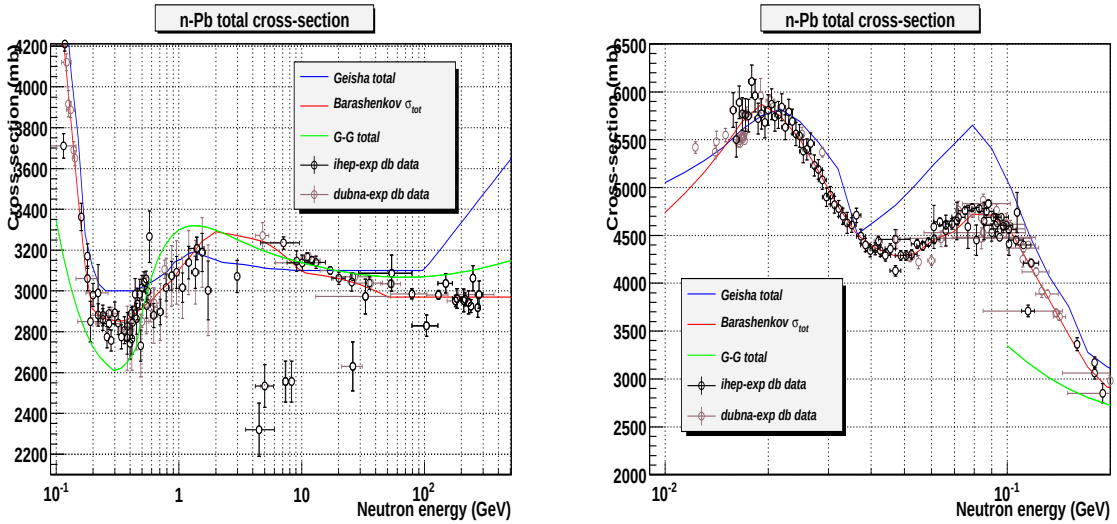

(a) (b)

Figure 13: Integral total cross-sections of neutrons on lead target: (a) - $10^{-1} - 500$ GeV, (b) - $10^{-2} - 0.2$ GeV. Experimental data (open points) from [7, 8], lines correspond to different GEANT4 models.

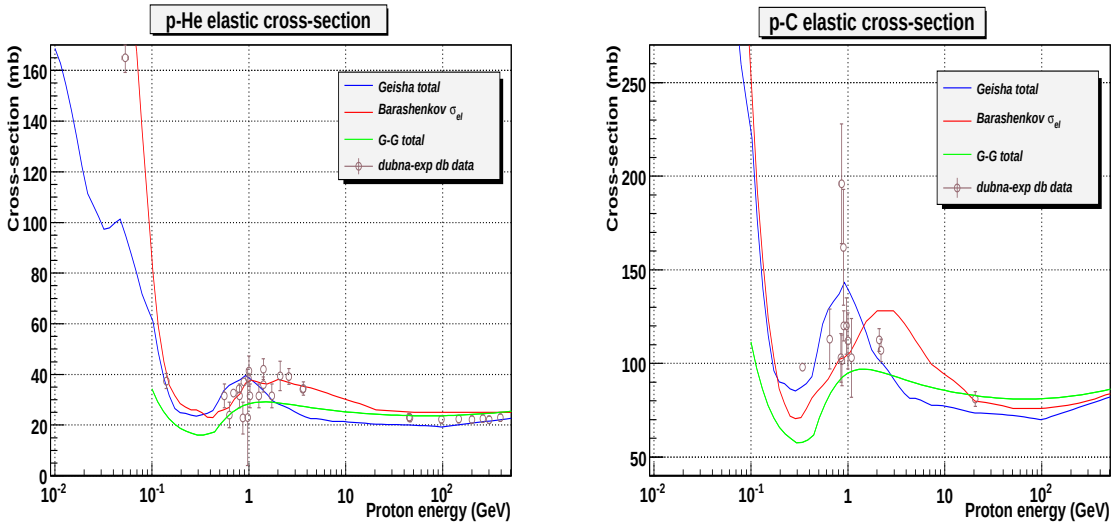

(a) (b)

Figure 14: Integral elastic cross-sections of protons on helium (a) and carbon (b) targets. Experimental data (open points) from [7, 8], lines correspond to different GEANT4 models.

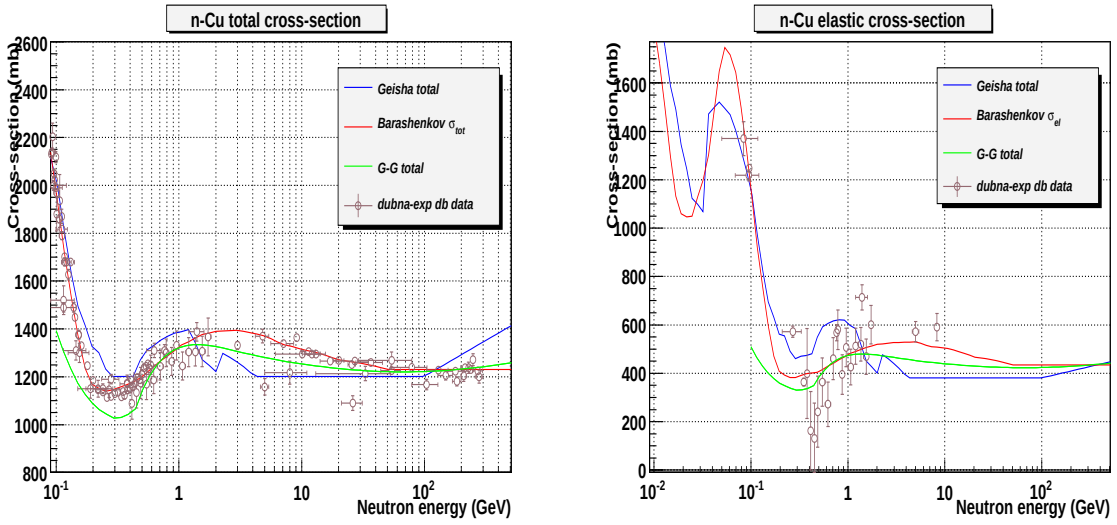

(a) (b)

Figure 15: Integral total (a) - $10^{-1}-500$ GeV and elastic (b) cross-sections of neutrons on carbon target. Experimental data (open points) from [7, 8], lines correspond to different GEANT4 models.

5 Conclusions

The following conclusions can be made from the comparison with experimental data:

1. G4Pi/NucleonNuclearCrossSection classes based on Barashenkov parametrization show good agreement with experimental data for total, inelastic and elastic cross sections in the wide energy range 10 MeV - 1 TeV.

2. Simplified Glauber model can be used as prolongation of Barashenkov cross sections for the energy range $>$ 100 GeV.

3. Simplified Glauber model was extended for the description of h-A production and single-diffraction cross sections.

4. The quasi-elastic/inelastic and single-diffraction/inelastic cross section ratios are available for different projectiles and targets. They are in qualitative agreement with CHIPS predictions in the energy range 1-100 GeV.

Acknowledgement

This work is supported by the Commission of the European Communities under the 6^{th} Framework Program "Structuring the European Research Area", contract number RII3-026126. The authors are thankful to J. Apostolakis, D. Wright and other members of GEANT4 hadronic group for fruitful discussions and help.

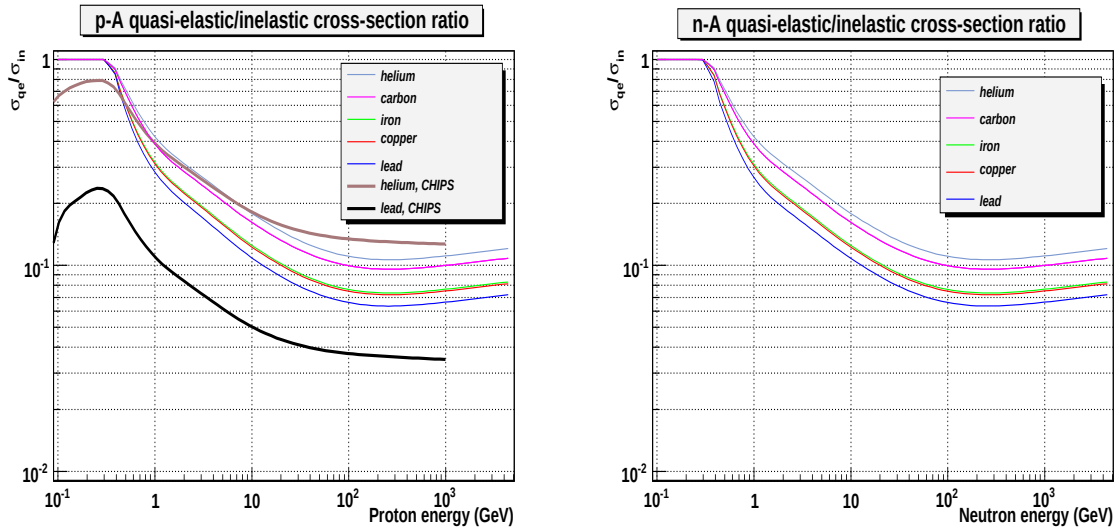

(a) (b)

Figure 16: Quasi-elastic to inelastic cross-section ratios for protons (a) and neutrons (b) on different targets. Thick lines correspond to the prediction of CHIPS parametrization.

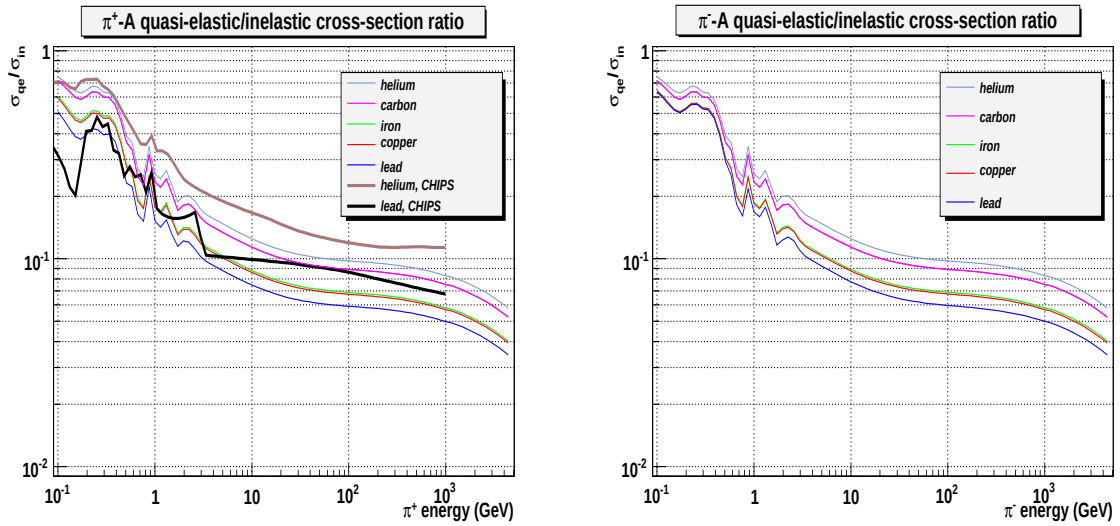

(a) (b)

Figure 17: Quasi-elastic to inelastic cross-section ratios for π^+ (a) and π^- (b) on different targets. Thick lines correspond to the prediction of CHIPS parametrization.

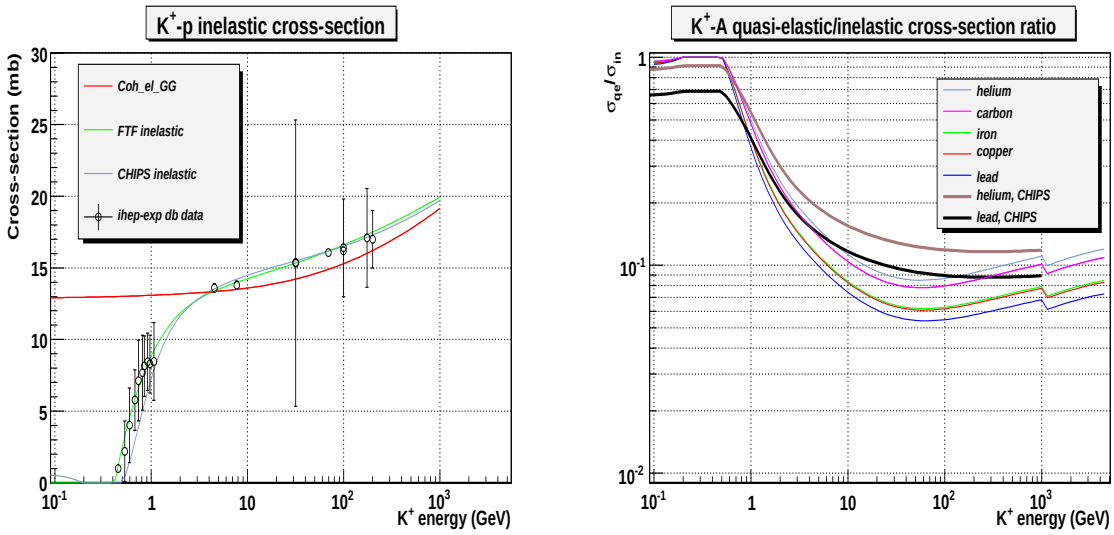

(a) (b)

Figure 18: Different GEANT4 parameterizations for K^+p inelastic cross-section (a) and quasi-elastic to inelastic cross-section ratios for K^+ (b) on different targets. Thick lines correspond to the prediction of CHIPS parametrization.

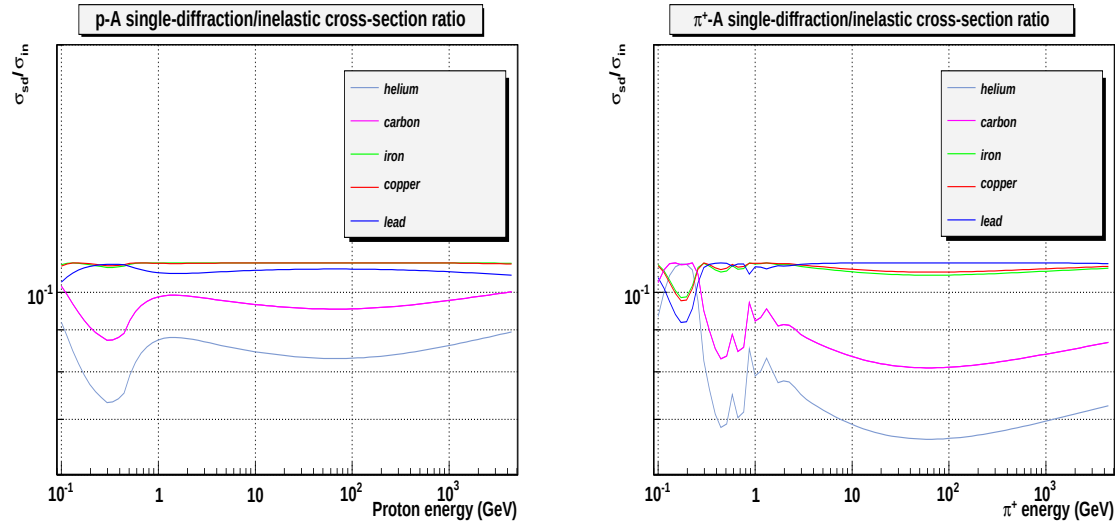

(a) (b)

Figure 19: Single-diffraction to inelastic cross-section ratios for protons (a) and π^+ (b) on different targets.

References

[1] GEANT4 Collaboration, GEANT4 : A Simulation Toolkit, *Nucl. Instr. and Meth.* **A506** 250 (2003); see also http://cern.ch/geant4/.

[2] H. Fesefeld, The Simulation of Hadronic Showers, Preprint PITHA 85/02.

[3] H.P. Wellisch, D. Axen, Total reaction cross sections in proton-nucleus scattering, *Physical Review* **C54** (1996) 1329-1332.

[4] P. V. Degtyrenko, M. V. Kossov and H.P. Wellisch, Eur. Phys. Journ., A8 (2000) 217.

[5] V.S Barashenkov, Pion-Nucleus Cross-sections, Preprint P2-90-158, Dubna 1990.

[6] V.S Barashenkov, Nucleon-Nucleus Cross-sections, Preprint P2-89-770, Dubna 1989.

[7] http://wwwppds.ihep.su.

[8] http://wwwnea.fr/html/dbdata/bara.html.

[9] B.Z. Kopeliovitch, Transparent Nuclei and Deuteron-Gold Collisions at HRIC, nucl-th/0306044, Sep 5 , 2003.

[10] http://pdg.lbl.gov/2006/reviews/hadronicrpp.pdf.